JPE 18-5-16

https://doi.org/10.6113/JPE.2018.18.5.1470
ISSN(Print): 1598-2092 / ISSN(Online): 2093-4718

Improved Particle Swarm Optimization Algorithm for Adaptive Frequency-Tracking Control in Wireless Power Transfer Systems

Yang Li*, Liu Liu†, Cheng Zhang*, Qingxin Yang*, Jianxiong Li*, Xian Zhang*, and Ming Xue*

†,*Tianjin Key Laboratory of Advanced Electrical Engineering and Energy Technology, Tianjin Polytechnic University, Tianjin, China

Abstract

Recently, wireless power transfer (WPT) via coupled magnetic resonances has attracted a lot of attention owing to its long operation distance and high efficiency. However, the WPT systems is over-coupling and a frequency splitting phenomenon occurs when resonators are placed closely, which leads to a decrease in the transfer power. To solve this problem, an adaptive frequency tracking control (AFTC) was used based on a closed-loop control scheme. An improved particle swarm optimization (PSO) algorithm was proposed with the AFTC to track the maximum power point in real time. In addition, simulations were carried out. Finally, a WPT system with the AFTC was demonstrated to experimentally validate the improved PSO algorithm and its tracking performance in terms of optimal frequency.

Key words: Adaptive frequency tracking, Improved particle swarm optimization algorithm, Over coupling, Wireless power transfer

I. INTRODUCTION

When compared with inductive coupling, coupled magnetic resonance uses a weak magnetic field but it can be transferred over a greater distance [1]-[4]. It also has the characteristics of non-radiation and security in comparison with radio waves, and the designs of transmitter and receiver are simpler [5]. However, wireless power transfer (WPT) via coupled magnetic resonances is still in its infancy [6], [7]. Theoretic and experimental analysis are lacking. In addition, there are many problems to be solved, especially the reduction of transfer power in the case of over coupling. When the transmitter and receiver are placed so close that the coupling condition is greater than the critical coupling, the single resonant peak at the load splits into double peaks [8]. Once the frequency splitting phenomenon occurs, the transfer power drops rapidly [9]. An adaptive frequency tracking control (AFTC) method, which tracks the splitting frequency to harvest the maximum transfer power by adaptively changing the operation frequency of the power source, is a promising approach to alleviate the reduction of transfer power in the presence of gap variations.

At present, the technology for frequency-tracking is mature. In [10], the frequency-tracking of load current was implemented by a phase lock loop (PLL), and an automated frequency-tracking control system was realized by introducing a phase-compensated circuit. In [11], a wireless power transfer system with resonant coupling was presented based on a PLL to achieve frequency-tracking at a frequency higher than 1MHz. In [12], an optimum frequency-tracking algorithm used the power transfer efficiency of a wireless power link. In addition, a power amplifier was introduced into an automated frequency-tracking system. In [13], the transfer power was improved by tracking the inverter frequency and adjusting the capacities according to the coupling change. These studies have made a great deal of progress in frequency-tracking. However, the speed of the frequency-tracking, which is key for moving devices, was not considered in the above studies.

There are also many studies based on improved particle swarm optimization (PSO) algorithms. In [14], a chaos PSO algorithm combined with multi-agent scheme was presented

Manuscript received July. 5, 2017; accepted May. 4, 2018
Recommended for publication by Associate Editor Hao Ma.
†Corresponding Author: liuliulovefly@163.com
Tel: +86-22-83955414, Tianjin Polytechnic University
*Tianjin Key Laboratory of Advanced Electrical Engineering and Energy Technology, Tianjin Polytechnic University, China

for the dynamic positioning system of a vessel. In [15], an adaptive inertial weight PSO algorithm was introduced to improve the maximum power point tracking capability of a photovoltaic system. In [16], an improved PSO algorithm was employed for density control in freeway mainlines. It should be noted that the above studies seldom refer to WPT systems.

In this paper, an improved PSO algorithm that adaptively changes the inertia weight is proposed to implement an AFTC in a WPT system, which can track the maximum power point in real time. Moreover, AFTC achieves the feedback of the required frequency based on a closed-loop control scheme, which significantly improves the transfer power.

The rest of this paper is organized as follows. A WPT system with an AFTC is analyzed in Section II, and an improved PSO algorithm is proposed in Section III. In Section IV, the characteristics of the AFTC based on the improved PSO algorithm are simulated. Some experiments are reported in Section V, and conclusions are given in Section VI.

II. Overview of an Adaptive Frequency - Tracking System

Before the design of an adaptive frequency-tracking system, the properties of a WPT system are analyzed through simulation. The WPT system consists of two identical round copper loop resonators (exterior dimension: 34.1cm×2.1mm× 2.1cm; coil impedance: 48+j0.5Ω), i.e., a transmitter and a receiver, and they are tuned with lumped capacitors at 4.525MHz. When the two resonators are placed within a distance range of 10 cm, the resonant frequency is split into odd and even modes [17]. The input resistances of both operating modes are obtained from simulations when a 50 Ω load is connected to the receiving side. Therefore, without an exterior impedance matching circuit, tracking the resonance frequency is equivalent to reasonable impedance matching at 50 Ω.

A WPT system with an AFTC is shown in Fig. 1, where a monolithic integrated DDS is used to generate a sinusoidal signal of high frequency. However, the energy of the signal is so small that it is impossible to be used in the WPT system. Therefore, the signal is enlarged by a power amplifier, which is further transferred to the receiver through resonators. The high frequency alternating current of the signal is rectified through a full-wave bridge rectified filter, and the voltage is processed by a stabilized voltage circuit. In the end, power is supplied to the load. Meanwhile, a power detection module is used to process the voltage and current signals, and the results are transferred to a DSP. The improved PSO algorithm embedded in the DSP is triggered by the results, and then it outputs the optimal frequency to a DDS. The DDS generates a sinusoidal signal of optimal frequency, which can maximize the transfer power.

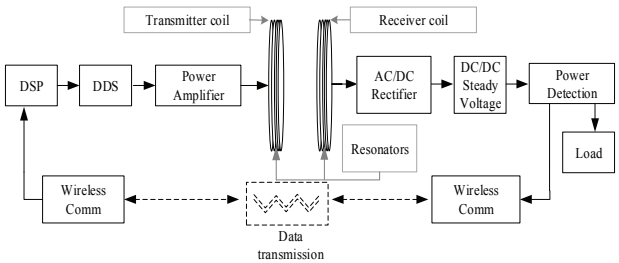

Fig. 1. WPT system with an AFTC.

III. Improved Particle Swarm Optimization Algorithm

A. Standard PSO Algorithm

The standard PSO algorithm is a highly efficient and parallel optimization method that can be used to solve nonlinear optimization problems. When compared with a genetic algorithm (GA), it has a faster running speed, a smaller number of calculations and fewer adjustable parameters. Hence, it is widely applied in engineering fields.

For particle i, its position is expressed as $X^i=(x_{i,1}, x_{i,2}, \ldots, x_{i,d})$, and its velocity is $V^i=(v_{i,1},v_{i,2}, \ldots, v_{i,d})$. The best position for particle i is $P^i=(p_{i,1},p_{i,2}, \ldots, p_{i,d})$, and it is called p_{best}. Another best place is called g_{best}, which represents the global best position for all of the particles. The particles modify their moving speeds and positions according to equations (1) and (2).

$$v_{i,j}(t+1)=wv_{i,j}(t)+c_1r_1\left[p_{i,j}-x_{i,j}(t)\right]+c_2r_2\left[p_{g,j}-x_{i,j}(t)\right] \quad (1)$$

$$x_{i,j}(t+1)=x_{i,j}(t)+v_{i,j}(t), j=1,2,\ldots,d \quad (2)$$

where t denotes iterative time, d stands for the total number of dimensions, and ω denotes the inertia weight value. The parameters c_1 and c_2 are learning factors, and they are also called acceleration coefficients. The variables r_1 and r_2 are random numbers between 0 and 1.

B. Improved PSO Algorithm

1) Chaos Initialization: For the globally convergent PSO algorithm, the initial population is an important factor that affects its convergence [18]. Because it is impossible to determine the space of the best solution in the initial searching stage, the value of the initial population can only be used to represent the feature of the solution space. If the choice of the initial population is better, the algorithm quickly reaches the global optimum after a number of iterations. Otherwise, it may reach the local optimum in the beginning, which affects the global convergence. In order to solve this problem, scholars have put forward various solutions [19], [20]. In this paper, an adaptive PSO algorithm combined with chaotic map is proposed, where a piecewise logistic chaotic map is used to generate the position and velocity of the initial

population [21]. There are mainly three steps as follows:

Step 1. Firstly, two 1×D random vectors that represent the position X1 and the velocity V1 of the first particle are generated, and all of the values of the random vectors are between 0 and 1.

Step 2. Equations (3) and (4) are used to generate 2*(N-1) vectors by a number of iterations. They represent the positions X2 , X3 , ... , XN and velocities V2 , V3 , ... , VN of the remaining (N-1) particles in the initial population.

$$x_{i+1,d}=\begin{cases}16*x_{i-1,d}*\left(0.5-x_{i-1,d}\right) & , \quad 0<x_{i-1,d}<0.5\\ 1-16*\left(1-x_{i-1,d}\right)*\left(x_{i-1,d}-0.5\right) & , \quad 0.5\le x_{i-1,d}<1\end{cases} \tag{3}$$

$$v_{i+1,d}=\begin{cases}16*v_{i-1,d}*\left(0.5-v_{i-1,d}\right) & , \quad 0<v_{i-1,d}<0.5\\ 1-16*\left(1-v_{i-1,d}\right)*\left(v_{i-1,d}-0.5\right) & , \quad 0.5\le v_{i-1,d}<1\end{cases} \tag{4}$$

Step 3. In a WPT system with an AFTC, the critical coupling distance is 15 cm, which is obtained from experimental measurements. When the distance between transmitter coil and receiver coil is 15 cm, the transfer power reaches its maximum because the input impedance of system is 50 Ω, which is exactly matched with the characteristic resistance of the power amplifier. When the distance between resonators is 10 cm, the system is over-coupling, and the frequency splitting phenomenon occurs. Then the maximum power is obtained at the splitting points, which are distributed in the range of 3.3-5.5MHz. However, the initial values are generated in the range of (0, 1) after the above two steps. Thus, it is necessary to map the initial positions and velocities to the specified search space (3.3,5.5) by equations (5) and (6) as follows:

$$x_{i,d}=4.4+\left(2*x_{i,d}-1\right) \tag{5}$$

$$v_{i,d}=4.4+\left(2*v_{i,d}-1\right) \tag{6}$$

2) Adaptive Change of Inertia Weight: The value of inertia weight value ω plays a significant role in the convergent effect of the PSO algorithm. In the standard PSO algorithm, it is used to control the influence of the history velocities on the current velocity, and to keep a balance between a global search and a local search. A bigger inertia weight value helps to increase the value of $\omega\cdot v_{i,j}$, enlarge the search space, improve the ability of the global search and increase the population diversity. On the other hand, a smaller inertia weight value helps weaken the search space of the velocity, improve the capability in terms of searching for the best solution locally and accelerate the convergence of the algorithm. In the standard PSO algorithm, ω generally decreases linearly with an increase in the number of iterative times. Note, there are some problems in this method. Firstly, if the best position is detected in an early stage, it is expected

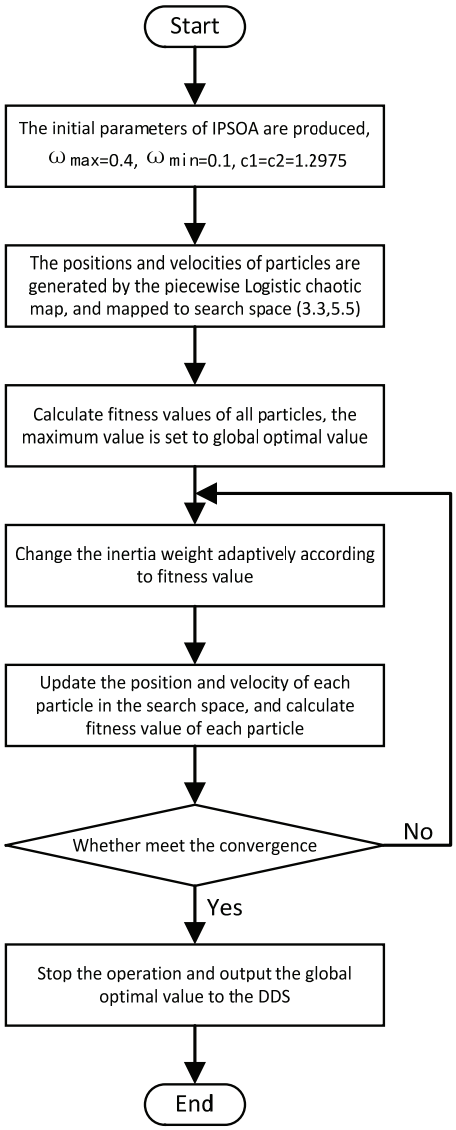

Fig. 2. Flowchart of the improved PSO algorithm.

to converge to the global optimum. However, a linear decrease of ω slows the convergence speed of the algorithm. Secondly, with a decrease of inertia weight, the capability of a global search decreases and the population diversity is weakened, which causes the algorithm is to easily fall into a local optimum in a later stage. To overcome the above problems, an improved formula of the inertia weight is expressed as follows:

Where, ω_{max} and ω_{min} represent the maximum and minimum values of the inertia weight, respectively. In addition, f , which

$$\omega=\begin{cases}\omega_{min}-\dfrac{\left(\omega_{max}-\omega_{min}\right)*\left(f-f_{min}\right)}{\left(f_{avg}-f_{min}\right)} & , \quad f\le f_{avg}\\ \omega_{max} & , \quad f>f_{avg}\end{cases} \tag{7}$$

is a fitness value of the particle, is fitted by using a Gaussian function in the simulation section. Meanwhile, f_{avg} and f_{min} are

the average fitness value and the minimum fitness value, respectively. They are updated in each iteration by equations (8) and (9).

$$f_{avg} = \frac{\sum_{i=1}^{N} f\left(x_{i,d}\right)}{N} \tag{8}$$

$$f_{min} = \min f\left(x_{i,d}\right), i = 1 \cdots N \tag{9}$$

Where N represent the number of particles. A flowchart of the improved PSO algorithm is shown in Fig. 2.

IV. Simulation Results

In this section, a simulation model is established in MATLAB/Simulink under the AFTC strategy. A large number of power points are sampled in the range of 3.3-5.5 MHz, which corresponds to a fixed distance of 10 cm (critical coupling distance: 15 cm). Then the curve of the power *vs* frequency is fitted using a Gaussian function by equation (10).

$$f = 8.753e^{-(x_{i,1}-4.497)/0.8898^2} + 2.653e^{-(x_{i,1}-4.993)/0.1007^2} - 403.5e^{-(x_{i,1}-4.965)/0.2937^2} + 31.65e^{-(x_{i,1}-4.618)/0.4505^2} + 129.7e^{-(x_{i,1}-4.86)/0.248^2} + 310e^{-(x_{i,1}-5.021)/0.2767^2} \tag{10}$$

Where f represents the load power and x represents the operation frequency. The fitting result is as follows: goodness of fit, 0.9974; R-square, 0.9995; adjusted R-square, 0.9988; and standard deviation, 0.3131. Therefore, the model agrees well with the actual experimental results.

In order to illustrate the advantages of the improved PSO algorithm, a standard PSO algorithm is simulated under the same conditions, i.e., the number of particles is 10; iteration time, 60; $c_1, c_2 \in [0,2]$, c_1=c_2=1.2975; and r_1 and r_2 are generated by random functions in each iteration. The simulation results are shown in Fig. 3.

In order to understand the iterative progress and the aggregation degree of the particles better, the denseness of the blue vertical line is used to indicate the iterative progress, and a denser area means that most of the particles converge quickly to the global optimum after the global optimum is found. The red point represents the fitness value of the particle, and the denseness of these points indicates the aggregation degree of the particles. The big black point represents the maximum fitness value, and the specific value and its corresponding frequency are labelled in the box. When compared with the actual resonant frequency (4.5 MHz), the operation frequency (4.455 MHz) is obtained by the AFTC based on the standard or improved PSO algorithm, and the load power is 30.45 W at a distance of 10 cm. A comparison between the improved and standard PSO algorithms is shown in Fig. 4.

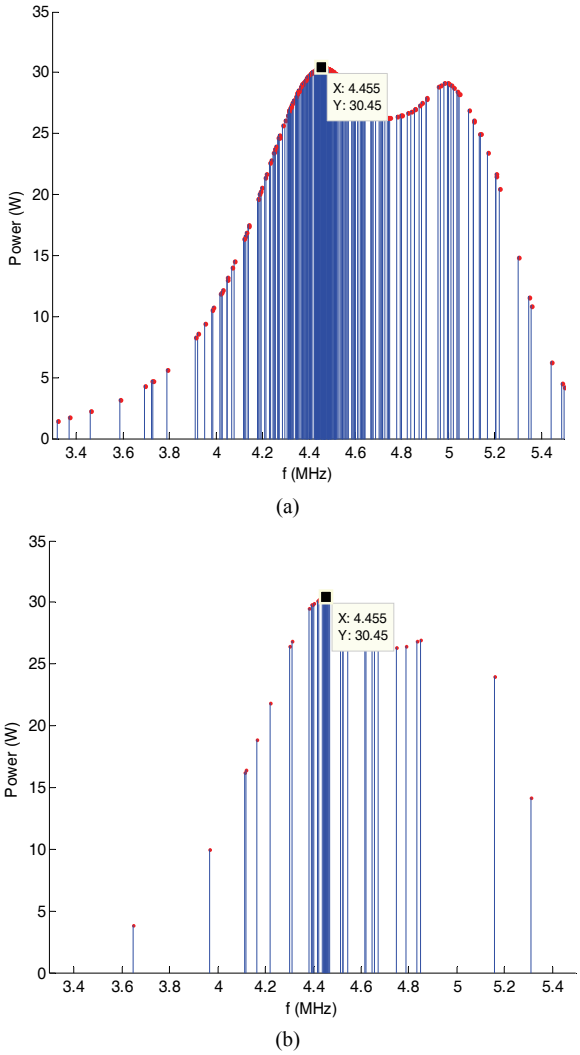

Fig. 3. Simulations results of: (a) Standard PSO algorithm, (b) Improved PSO algorithm.

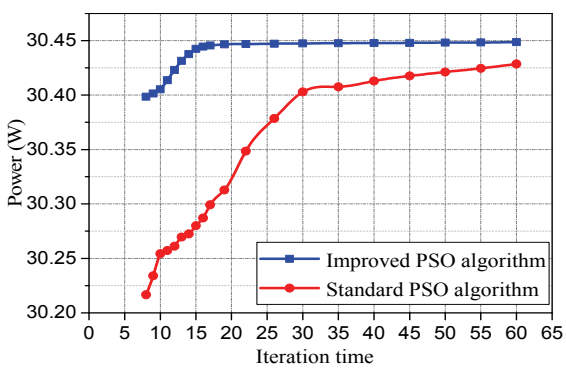

Fig. 4. Comparison between the improved and standard PSO Algorithms.

It can be clearly seen that the improved PSO algorithm has advantages in terms of tracking performance and convergence speed, e.g., it finds a global optimum solution at the value of 30.45 after 20 iterations. In comparison, the standard algorithm needs over 50 iterations to reach the maximum value.

TABLE I
PARAMETERS OF THE FOUR-COIL STRUCTURE

Parameter	Transmitting coil	Receiving coil	Transmitter resonant coil	Receiver resonant coil
Inductance (μH)	1.850	1.800	70.20	68.90
Capacitance (pF)	685.2	685.0	17.60	17.90
Resistance (Ω)	1.800	1.760	50.13	49.87
Turn (coil)	1.000	1.000	10.00	10.00
Diameter (cm)	17.05	17.05	17.05	17.05
Wire Diameter (mm)	2.100	2.100	2.100	2.100
Resonant Frequency (MHz)	4.470	4.533	4.528	4.532

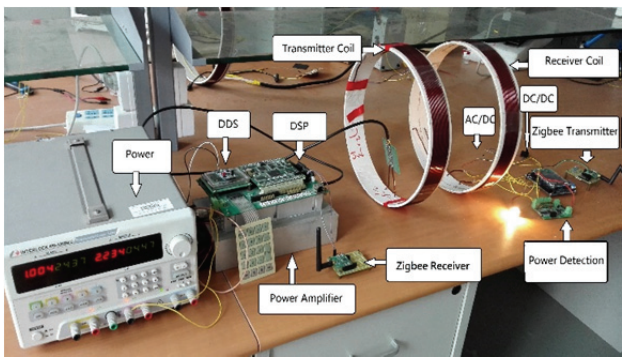

Fig. 5. Experimental platform.

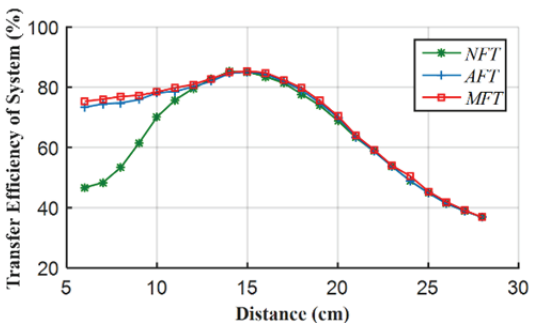

Fig. 6. Transfer efficiency of the system under the NFT, AFT and MFT.

V. EXPERIMENT RESULTS

Based on the simulation, a WPT system with the AFTC experimental platform was established, as shown in Fig. 5. The system is mainly composed of a power supply, DSP, DDS, power amplifier, resonators, rectifier circuit, power detection, wireless communication modules and load. Where the power supply provides the working voltage for the DDS, DSP and power amplifier, so they can produce a high frequency excitation signal for the resonators. Then the power detection converts the RF power signal into a voltage signal, which is transmitted to the DSP by a ZigBee transceiver module. Note that the working frequency of the ZigBee is 2.4GHz, which is different from the resonance frequency of the WPT system. As a result, it has no influence on the transmission performance of the system. Then the voltage signal is converted into a power value by the DSP and the optimal frequency of the system is obtained from the improved PSO algorithm. The parameters of the four-coil structure are listed in Table I.

A. The effect of the AFTC based on the Improved PSO on the System Efficiency

The measured transfer efficiency of the system comparisons under no frequency tracking (NFT), adaptive frequency tracking (AFT) and manual frequency tracking (MFT) for various distances are presented in Fig. 6. The MFT means that the working frequency of the DDS is manually adjusted for frequency scanning. Then the maximum value of the load power and the optimal frequency are found in the case of over- coupling. The MFT, which is the best way to achieve frequency tracking, can significantly improve the load power and track the optimal frequency accurately. However, this way is not suitable for intelligent WPT systems because it takes more time and needs manual operation. The transfer efficiency of the system is obtained based on the power measured at the resonators of the transmitter and the receiver. In a WPT system without frequency tracking, when the distance is initially set to 15 cm, the transfer efficiency of system is around 85.13%. However, the efficiency drops abruptly at other distances due to impedance mismatch. In the WPT system with frequency tracking, the transfer efficiency is improved significantly when the distance is less than 15 cm. In this case, more than 70% efficiency can be achieved. Although the transfer efficiency of the system is degraded with increasing distance due to the power transfer propagation properties, the improvement of the transfer efficiency over a distance from 6 to 15 cm is consistently achieved as shown in the Fig. 6.

B. Comparison of Algorithms in Terms of Tracking Speeds

In order to compare the frequency-tracking performance among the different search algorithms that include the improved PSO algorithm, standard PSO algorithm and standard genetic algorithm, experiments have been performed according to the scenarios illustrated in Fig. 7 (a). With an initial transmission distance of 15 cm. The distance is changed to 12 cm at MOVE I, and it is changed to 10 cm at

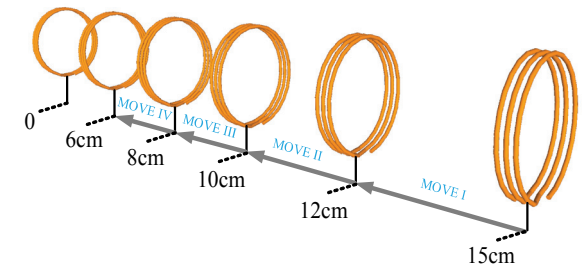

(a)

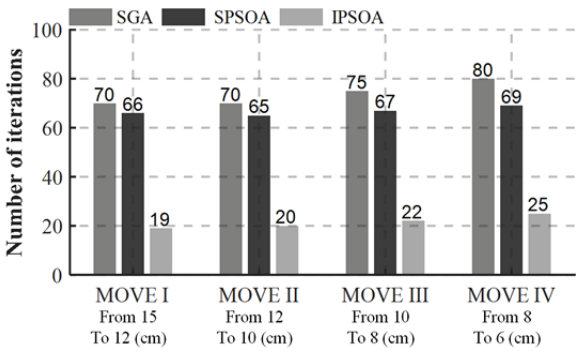

(b)

Fig. 7. Illustrations of: (a) Different scenarios for measuring the tracking performance of the improved PSO algorithm (IPSOA), standard PSO algorithm (SPSOA) and standard GA (SGA), (b) Number of iterations taken to obtain the optimal frequency under different scenarios when three different algorithms are used.

MOVE II. In the four cases (MOVE I to MOVE IV) specified in Fig. 7 (b), the optimal frequency is obtained using three different tracking approaches, and the tracking performances are compared. Obviously, when compared with the standard PSO algorithm and the genetic algorithm, the improved PSO algorithm has the least number of iterations, which means that the AFT takes the least time. Therefore, it can track the optimal frequency and achieve the maximum load power more quickly.

In addition, waveforms of the output voltage of the signal source through the iterative process of the AFTC based on IPSOA were recorded when the transfer distance was form 15 cm to 12 cm (i.e., MOVE I), as shown in Fig. 8. Moreover, the second half of the iteration process was recorded to illustrate this more clearly. As can be seen, since the system detected a decrease in power, it began to iterate the frequency according to the instructions of the IPSOA to track the optimal frequency. With an increase in the number of iterations, the system frequency gradually stabilized to the optimal operating frequency. At this frequency, the system power was an extreme value at the same transfer distance versus frequencies, which illustrates the effectiveness of the algorithm.

In addition, the normalized power versus frequency and transfer distance was drawn through a mathematical model. It recorded stable waveforms of the output voltage of the signal

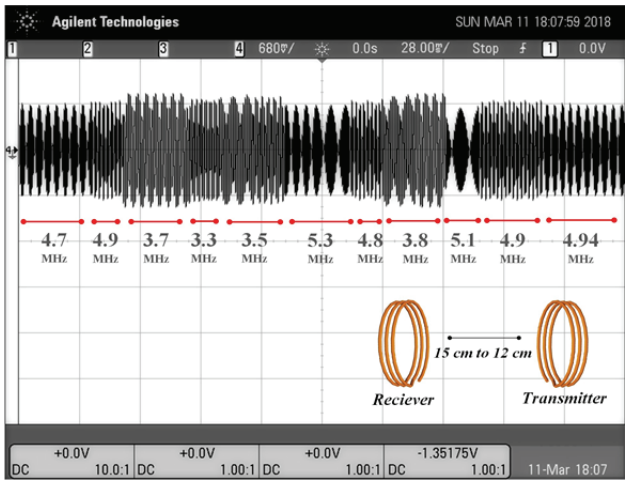

Fig. 8. The waveforms of the output voltage of the DDS through iterative process of the AFTC based on IPSOA.

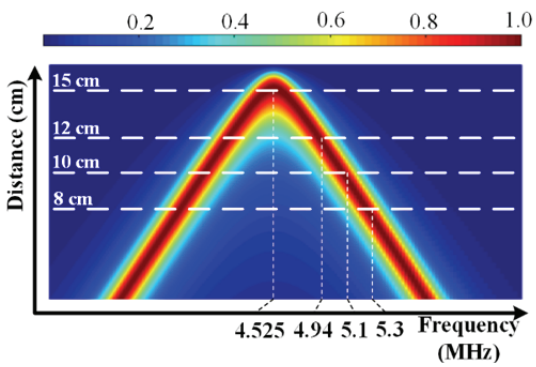

(a)

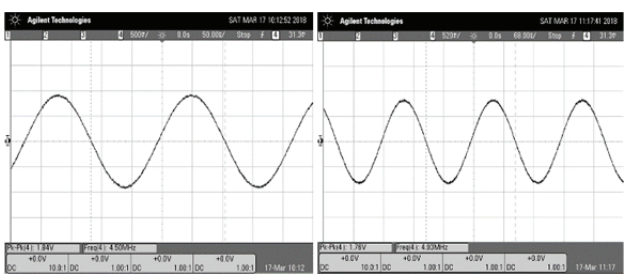

(b) (c)

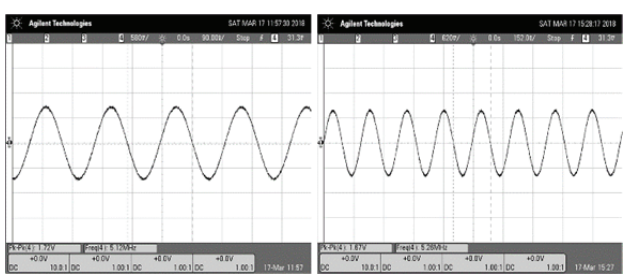

(d) (e)

Fig. 9. Illustrations of: (a) Normalized power versus frequency and transfer distance of the coils, where the color-bar represents the normalized power with the red indicating a higher power received by the load. Stable waveforms of the output voltage of the DDS with the following transfer distances: (b) 15 cm, (c) 12 cm, (d) 10 cm, (e) 8 cm.

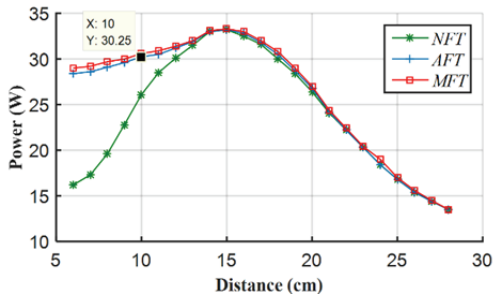

Fig. 10. Load power under NFT, AFT and MFT.

TABLE II
STATISTICAL RESULTS

Tracking way	Sample capacity	Mean value	Standard deviation	Stand error of mean
MFT	23	26.5817	6.5157	1.3586
AFT	23	26.2849	6.4991	1.3550

TABLE III
TEST RESULTS OF VARIANCE HOMOGENEITY WITH THE AFT

Hypothesis testing	*F*-value	Significance	*T*-value
Set-equal variance	0.01	0.976	0.157
Double-tail significant	Mean difference	Standard error values	
0.876	0.30174	1.91896	

source when the transfer distances were 15 cm, 12 cm, 10 cm, and 8 cm, respectively, as shown in Fig. 9. As can be seen, with the distance decreased, the system frequency gradually increased as well (note: in order to optimize the optimizing speed, the searching space of the algorithm was set to be higher than the natural resonance frequency of the coil). In addition, the system can accurately adjust the operating frequency through the algorithm and make the system transmission power reach an extreme peak value, which verifies the effectiveness of the proposed algorithm.

C. *The effect of the AFTC based on the Improved PSO on Transfer Power*

To further illustrate the performance of the proposed improved PSO algorithm, three groups of experiments were carried out. Curves describing the relationship between the load power and the distance between the transmitter and the receiver are shown in Fig. 10.

The maximum power of the NFT curve appeared at 15 cm. However, the load power became smaller when the distance was shorter. The maximum power of the MFT appeared at the same distance, while its load power was improved significantly when the distance was shorter. The big black point represented the value of the load power at 10 cm, and the specific value and corresponding distance were labelled in the box. The AFT curve was basically the same as the middle curve. However, all of its values were slightly larger than those of the MFT in the case of over coupling. These experimental results indicates that frequency tracking is the key to the transfer power in the case of over coupling and that the AFT control method is effective in improving the power.

The statistical results of the MFT and AFT are listed in Table II. The mean values of the MFT and AFT are 26.5817 and 26.2849, respectively. In addition, the maximum errors are both within 5.00%.

The test results of the variance homogeneity with the AFT based on the improved PSO algorithm are listed in Table III. The F value is 0.001, and the significance probability is 0.976, which indicate that there is no significant difference between the variances of the AFT and MFT. The double-tailed significant test is 0.876, which is greater than 0.05. This indicates that there is no significant difference between the means of the MFT and AFT under the 95% confidence interval of the mean difference. In a word, the above data analysis shows that the AFT based on the improved PSO algorithm can alleviate the attenuation of power against distance variations in the case of over coupling, just like the MFT.

VI. CONCLUSION

In this paper, an improved PSO algorithm was proposed, and inertia weight was adaptively adjusted under a nonlinear dynamic weighting control strategy. Simulation results based on MATLAB verified the algorithm. A comparison of the improved PSO algorithm, the standard PSO algorithm and a genetic algorithm showed that the improved algorithm can track the optimal frequency quickly and accurately. Moreover, the improved PSO algorithm with AFTC can change the operating frequency to track the maximum power point in real time. Experimental analysis of three tracking ways verified that the AFT based on the improved PSO algorithm can basically achieve the same effect as the MFT, which can improve the transfer power in the case of over coupling.

ACKNOWLEDGMENT

This work was supported by the National Natural Science Foundation of China under Grant [number 51577133], [number 51477117], [number 51607121]; Tianjin Research Program of Application Foundation and Advanced Technology under Grant [number 15JCYBJC46700]; National Key Research and Development Program of China under Grant [number 2017YFB1201003-022]; and Program for Innovative Research Team in University of Tianjin under Grant [number TD13-5040].

REFERENCES

[1] Q. X. Yang, H. Y. Chen, G. Z. Xu, M. G. Sun, and W. N. Fu, "Research progress in contactless power transfer technology," *Trans. China Electrotechnical Soc.*, Vol. 25, No. 7, pp. 6-13, Jul. 2010.

[2] W. Z. Fu, B. Zhang, D. Y. Qiu, and W. Wang, "Maximum efficiency analysis and design of self-resonance coupling coils for wireless power transfer system," *Proc. CSEE*, Vol. 29, No. 18, pp. 21-26, Jun. 2009.
[3] Y. Sun, C. Y. Xia, X. Dai, and Y. G. Su, "Analysis and optimization of mutual inductance for inductively coupled power transfer system," *Trans. China Electrotechnical Soc.*, Vol. 30, No. 33, pp. 44-50, Nov. 2010.
[4] J. H. Zhang, X. L. Huang, Y. W. Zhou, and Y. Bo, "Feasibility of ultrasonic wireless power transmission," *Advanced Tech. Elect. Eng. Energy*, Vol. 30, No. 2, pp. 66-69, Apr. 2011.
[5] T. Takagaki, T. Yamamoto, K. Fujimori, M. Sanagi, and S. Nogi, "Efficient design approach of MW-class RF-DC conversion rectenna circuits by FDTD analysis," in *Proc. Asia-Pacific Microwave Conf.*, pp. 1945-1948, 2006.
[6] R. E. Hamam, A. Karalis, J. D. Joannopoulos, and M. Soljačić, "Coupled-mode theory for general free-space resonant scattering of wave," *Physical Rev.*, Vol. 75, No. 5, pp. 1-5, May 2007.
[7] A. Karalis, J. D. Joannopoulos, and M. Soljačić, "Efficient wireless non-radiative mid-range energy transfer," *Ann. of Physics*, Vol. 323, No. 1, pp. 34-38, Jan. 2008.
[8] A. Kurs, A. Karalis, R. Moffatt, J. D. Joannopoulos, and P. Fisher, M. Soljačić, "Wireless power transfer via strongly coupled magnetic resonances," *Science*, Vol. 317, No. 5834, pp. 83-86, Jun. 2007.
[9] Y. Li, Q. X. Yang, Z. Yan, H. Y. Chen, X. Zhang, L. Jin, and M. Xue, "Characteristic of frequency in wireless power transfer system via magnetic resonance coupling," *Electric Machines and Control*, Vol. 16, No. 7, pp. 7-11, Jul. 2012.
[10] L. S. Xiong and Y. J. Quan, "Application of CD4046 in induction heating power source," *Electric Welder*, Vol. 6, No. 14, pp. 14-16, Jun. 2000.
[11] W. Z. Fu, B. Zhang, and D. Y. Qiu, "Study on frequency-tracking wireless power transfer system by resonant coupling," in *Power Electron. and Motion Control Conf.* pp. 2658-2663, 2009.
[12] N. Y. Kim, K. Y. Kim, and Y. H. Rju, "Automated adaptive frequency tracking system for efficiency mid-range wireless power transfer via magnetic resonance coupling," in *Proc.42nd European Microwave Conf.*, pp. 221-222, 2012.
[13] B. Klaus, B. Lang, and T. Leibfried, "Technical analysis of frequency tracking possibilities for contactless electric vehicle charging," in *2014 IEEE Innovative Smart Grid Technologies*, pp. 577-582, 2014.
[14] G. C. Xu, D. W. Zhao, K. W. Zhang, and J. H. Ge, "Multi-agent chaos particle swarm optimization algorithm of thrust allocation for dynamic positioning vessels," in *2015 34th Chin. Control Conf.*, pp. 2389-2396, 2015.
[15] X. L. Yuan, D. F. Yang, and H. M. Liu, "MPPT of PV system under partial shading condition based on adaptive inertia weight particle swarm optimization algorithm," in *2015 IEEE Int. Conf. Cyber Technol in Automation, Control, and Intelligent Systems*, pp. 729-733, 2015.
[16] Q. Lu and X. R. Liang, "Freeway traffic density control based on improved particle swarm optimization algorithm," *in 2015 34th Chin. Control Conf.*, pp. 1117-1121, 2015.
[17] Y. Kim and H. Ling, "Investigation of coupled mode behavior of electrically small meander antennas," *Electron. Letters*, Vol. 43, No. 23, Nov. 2007.
[18] D. He, H. R. Chang, Q. Chang, and Y. Liu, "Particle swarm optimization based on the initial population of clustering," *in 2010 6th Int. Conf. on Natural Computation*, pp. 2664-2667, 2010.
[19] Y. Gao and S. L. Xie, "Chaos particle swarm optimization," *Computer Science*, Vol. 8, No. 31, pp. 13-15, 2004.
[20] H. Wang, Z. J. Wu, J. Wang, X. J. Dong, S. Yu, and C. Chen, "A new population initialization method based on space transformation search," in *2009 5th Int. Conf. Natural Computation*, pp. 332-336, 2009.
[21] Y. J. Xu, L. Chou, and Q. Liu, "Chaotic particle Swarm optimization with adaptive inertia weight," *J. Nanjing Univ. (Eng. Tech. Edition)*, No. 1, pp. 64-69, 2012.

Yang Li received his B.S., M.S. and Ph.D. degrees from the Hebei University of Technology, Tianjin, China, in 2002, 2005 and 2013, respectively. He is presently working as an Associate Professor in the School of Electrical Engineering and Automation, Tianjin Polytechnic University, Tianjin, China. His current research interests include wireless power transfer technologies.

Liu Liu was born in Handan, China, in 1993. She received her B.S. degree in Electrical Engineering from the Hebei Engineering University, Handan, China, in 2016. She is presently working towards her M.S. degree at the Tianjin Polytechnic University, Tianjin, China. Her current research interests include wireless power transmission.

Cheng Zhang was born in Anqing, China, in 1990. He received his B.S. degree in Electrical Engineering from the Zhengzhou University of Aeronautics, Zhengzhou, China, in 2014. He is presently working towards his M.S. degree in Electrical Engineering. His current research interests include wireless power transmission.

Qingxin Yang received his B.S., M.S. and Ph.D. degrees from the Hebei University of Technology, Tianjin, China, in 1983, 1986 and 1997, respectively. He is the President of the Tianjin Polytechnic University, Tianjin, China. His current research interests include electromagnetic field computation and wireless power transfer. Professor Yang is a Board Member of the International COMPUMAG Society and the President of the China Electrotechnical Society.

Jianxiong Li was born in 1969, in Tianjin, China. He received his B.S. and M.S. degrees in Physics, and his Ph.D. degree in Communication and Information Systems, from Tianjin University, Tianjin, China, in 1991, 1994 and 2007, respectively. His current research interests include computational electromagnetics, wireless power transfer and RFID antenna.

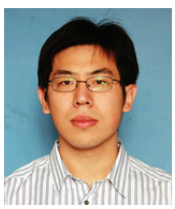

Xian Zhang received his B.S. and Ph.D. degrees from the Hebei University of Technology, Tianjin, China, in 2006 and 2012, respectively. He is presently working as an Associate Professor in the School of Electrical Engineering and Automation, Tianjin Polytechnic University, Tianjin, China. His current research interests include wireless power transfer.

Ming Xue received his B.S. and M.S. degrees from the Tianjin Polytechnic University, Tianjin, China, in 2011 and 2014, respectively. His current research interests include wireless power transmission.